LOW-ANGLE NORMAL FAULTS ON SATURN'S MOONS: EVIDENCE FOR VISCOUS RELAXATION.

C. B. Beddingfield[1], D. M. Burr[1], W. M. Dunne[1], [1]Earth and Planetary Sciences Department, University of Tennessee, Knoxville, TN, USA (cbeddin1@vols.utk.edu).

Introduction: Saturn's icy satellites commonly exhibit global scale sets of normal faults on their surfaces. Analyses of fault geometries can provide insight into tectonic behavior and the histories of these satellites. We investigate icy satellite normal fault geometries to determine if they exhibit dips consistent with those inferred from laboratory experiments.

Background: For icy satellite near-surface conditions, vertical normal stresses are small and temperatures are low, so fracture-related deformation is the expected behavior [1]. For brittle deformation, the material's coefficient of internal friction, μ_i, is related to the normal fault dip, δ_{normal} [2], where

$$\delta_{normal} = 45° + \frac{\arctan(\mu_i)}{2}. \quad (1)$$

This theory of brittle deformation may be applied to any material for which its μ_i is known, including cryogenic H_2O ice. Values for μ_i can be inferred from laboratory experiments for different materials, at various temperatures, confining pressures, and strain rates. Deformation experiment results for μ_i imply δ_{normal} on icy satellites should range from 45° to 59° [1,3,4].

Hypothesis: We investigate the premise that normal fault dips inferred from laboratory experiments are reflected on the surface of Saturn's satellites. We focus on fault geometries of three known global-scale extensional systems in the Saturnian system. These fault systems are Ithaca Chasma on Tethys, Avaiki Chasmata on Rhea, and the Wispy Terrain on Dione.

Data and Methods: To investigate fault scarp geometries, we generated and analyzed digital elevation models (DEMs) using the Softcopy Exploitation Toolkit (SOCET SET). The image pairs used for DEM generation were acquired by the Imaging Science Subsystem (ISS) camera onboard the Cassini spacecraft. These DEMs and images were exported to the Environmental Systems Research Institute's (ESRI's) ArcMap software for measurements and analyses.

Results: We find that most fault dips in the study areas are shallower than expectations from deformation experiments (Fig. 1). All scarps analyzed within Ithaca Chasma and Avaiki Chasmata exhibit dips below the expected range. In contrast, however, the average dips of most scarps analyzed within Dione's Wispy Terrain fall within the expected range. Thus, our hypothesis is not supported for Tethy's Ithaca Chasma on Tethys and Avaiki Chasmata on Rhea, but is supported for Dione's Wispy Terrain.

Analysis and Discussion: Terrestrial normal faults with dips <30° are termed low angle normal faults (LANFs) [5]. Proposed formation mechanisms for

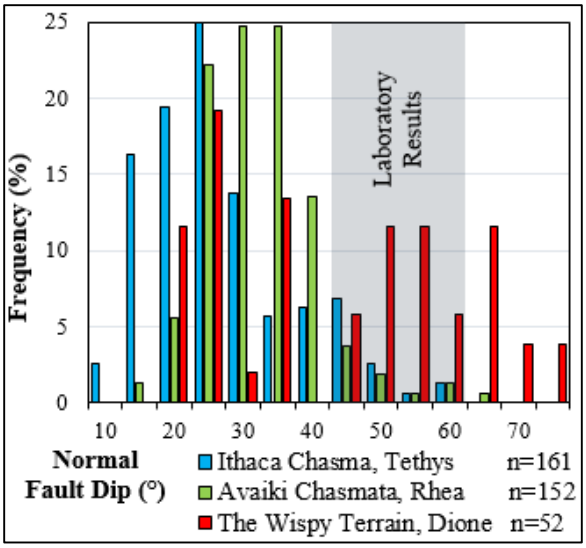

Figure 1: Fault dips measured in each study area are shown.

LANFs include fault rotation during offset [6], stress-axis perturbation [7], regolith deposition [8], and viscous relaxation [9].

Fault rotation during offset is an unlikely LANF formation mechanism in our study areas because the back-face slopes of the scarps are too shallow (<10°) to account for the low dips values. Stress-axis perturbation, a result of stresses introduced by topographic anomalies and intrusions, would likely produce dip variations between faults, but such variations are not observed. The scarp heights within Ithaca Chasma and the Wispy Terrain are much greater than the estimated regolith thicknesses on Tethys and Dione [10], suggesting regolith deposition is an unlikely explanation for LANFs. While Rhea's estimated regolith thickness is greater than some of the measured scarp heights of Avaiki Chasmata, it is less than other scarps heights. Consequently, regolith deposition is an unlikely explanation for LANF in these study areas.

Subdued impact crater topography on all three satellites has been interpreted to result from viscous relaxation [11]. Additional evidence for viscous relaxation on Tethys includes the presence of raised rims of Ithaca Chasma [12]. Consequently, viscous relaxation appears to be the most viable formation mechanism for LANFs that would be applicable in all three study areas.

Viscous Relaxation: We investigate the possible role of viscous relaxation for rotating moderately to steeply dipping normal faults into a geometry consistent with LANFs in our study areas. The relation of

initial scarp height, h_0, to the subsequent scarp height, h_t, is given by [13]

$$h_0 = h_t\, e^{\left(\frac{t}{\tau}\right)} \quad (2)$$

where

$$\tau = \frac{4\pi\eta}{\rho g \lambda} \quad (3)$$

and where density, ρ, and gravitational acceleration, g, are uniform, t is the age of the fault, η is mantle viscosity, and λ is the graben width. The initial fault dip formed at t=0, Θ_0, is given by

$$\theta_{0,degrees} = \left|\arctan\left(\frac{h_0}{w}\right)\frac{180°}{\pi}\right| \quad (4)$$

where w is the width of the scarp, assuming that w, when t>0, is approximately equal to w for t=0. The values for t are taken from age estimates for each study area [12,14,15]. We measure λ, w, *and* h_t for each fault scarp analyzed.

The effective mantle viscosity is given by

$$\eta = \left(\frac{d^p}{A}\right)\sigma_{diff}^{1-n}\exp\left(\frac{Q}{RT_Z}\right) \quad (5)$$

where d is the grain size, p, A, and n are empirical constants, σ_{diff} is the differential stress, Q is the activation energy of creep, R is the gas constant, and T_z is the temperature at the base of the satellite's lithosphere.

The grain size of the lithospheres of Tethys, Rhea, and Dione is unknown. We use estimates of the smallest grain size for Europa's lithosphere [16], as our grain size lower limit, and then consider grain sizes over an increase of two orders of magnitude. We use typical σ_{diff} values for tidal deformation and convection [17].

T_z , the basal lithospheric temperature, is given by

$$T_z = T_s e^{\frac{F z}{k}}, \quad (6)$$

where T_S is the surface temperature, F is heat flux, z is lithospheric thickness, and k is the thermal conductivity of H_2O ice. We use published estimates of T_s values [18,19] and F values [12,20-23] for each study area.

Estimates for z of Tethys [12] and Dione [24] are used. Because values for z have not been estimated for Rhea, we use the range of elastic thickness estimates to represent a minimum lithospheric thickness [21]. As shown in Eqs. 2-6, using the estimated range of elastic thicknesses will yield minimum magnitudes for the slope changes, since the elastic thickness is never greater than the lithospheric thickness. If calculations using elastic lithospheric thicknesses show viscous relaxation is a viable cause for the observed fault dips, this result would hold true if the greater lithospheric thickness values were known and used instead.

We calculate the average Θ_0 of LANFs in each study area (Eq. 4) using a range of calculated viscosities (Eq. 5) (Fig. 2). We find that Θ_0 could have been as steep as 90°, showing that viscous relaxation is a viable formation mechanism for these LANFs in all three study areas. Additional evidence for viscous relaxation of these regions are raised rims observed during this work of Avaiki Chasmata.

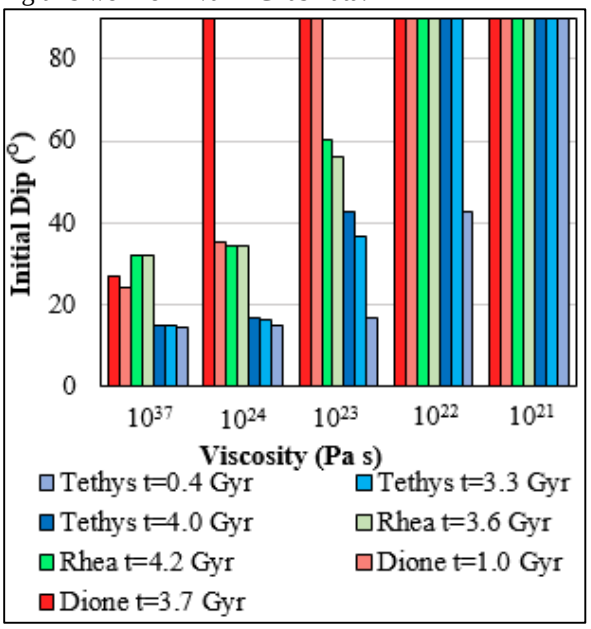

Figure 2: Estimated initial fault dips for analyzed LANFs in each study area.

Conclusions and Implications: We find that in the regions of Ithaca Chasma and Avaiki Chasmata, all measured normal fault dips are shallower than those inferred from cryogenic H_2O ice deformation experiments, and are inferred to be LANFs. Within Dione's Wispy Terrain, 75% of the faults exhibit dips within the expected dip range, while one fault is a LANF. We conclude that experimental behaviors applied at the time of faulting, but that fault geometry was subsequently modified by viscous relaxation.

References: [1] Durham et al. (1983) *JGR Sol. Ear., 88, B377-B392*. [2] Anderson (1951) *The Dynamics of Faulting and Dyke Formation*. [3] Beeman et al. (1988) *JGR Sol. Ear., 93, 7625-7633*. [4] Schulson and Fortt (2012) *JGR Sol. Ear. 117, B12*. [5] Wernicke et al. (1985) *Tect. 4, 213-246*. [6] Profett (1977), *GSA Bul., 88, 247-266*. [7] Spencer and Chase (1989), *JGR, 94, 1765-1775*. [8] Burbank and Anderson (2011) *Tectonic Geomorphology*. [9] Wernicke and Axen (1988). [10] Veverka (1986) *Satellites, 1, 342-402*. [11] P. Schenk and J. Moore. (2007) *LPS 38, 2305*. [12] Giese et al. (2007) *GRL, 34, 21*. [13] Cathles et al. (1975) *The Viscosity of the Earth's Mantle*. [14] Wagner et al. (2006) *LPS 37, 1805*. [15] Wagner et al. (2007) *LPS 38, 1958*. [16] Giessler et al. (1998) *Icarus, 135, 107-126*. [17] Tobi et al. (2003) *JGR 108, E11*. [18] Hanel at al. (1982) *Science, 215, 544-548*. [19] Cruikshank et al. (1984) *Saturn, 1, 640-667*. [20] Chen and Nimmo (2008) *GRL, 35, 19*. [21] Nimmo et al. (2010) *JGR 115, E10008*. [22] Hammond et al. (2013) *Icarus, 22, 418-422*. [23] White et al. (2013) *Icarus, 223, 699-709*. [24] Forni et al. (1991) *Icarus 94, 232-245*.